NANO · MICRO small
www.small-journal.com

Interplay of Depletion Forces and Biomolecular Recognition in the Hierarchical Assembly of Supramolecular Tubes

*Fangyuan Xiu, Anamarija Knežević, Jurriaan Huskens, and Tibor Kudernac**

Crowding effects have a profound impact on the hierarchical organization of cellular architectures. In the fields of systems chemistry and soft matter, this effect has not received much attention so far. Here, it is explored how poly(ethylene glycol) (PEG) as a crowding agent invokes depletion forces that act on synthetic supramolecular tubes. Hence, supramolecular tubes are pushed from their random orientation into hierarchically assembled bundles due to the PEG-induced crowded environment. The resulting morphology of formed bundled architectures can be tuned by the concentrations of both the supramolecular tubes and the PEG. The introduction of biotin groups at the surface of the tubes allows the engineering of biotin–streptavidin crosslinks between them. The order of introducing PEG and streptavidin in the system further affects the formed hierarchical assemblies, as well as their resistance toward dilution. The strategy described here provides a new route to establish hierarchically organized supramolecular architectures, combining crowding and specific biomolecular interactions, which shows the potential for controlling the structure of supramolecular materials and other soft matter systems.

1. Introduction

Complex hierarchical supramolecular fibers and filaments are ubiquitous in nature.[1] From DNA to chromatin,[2] and from proteins to collagen fibers,[3,4] they all assemble in a hierarchical fashion, and they span from the nanoscale to the microscale. These highly ordered structures exhibit essential functional properties for living systems. For instance, collagen-based structures confer mechanical properties to different types of tissues like skin, tendon, and bone. This functional diversity is attained by relying on the structural variation of supramolecular architectures comprised of just a few building blocks at distinct length scales, rather than through a large variety of building blocks.[3]

Hierarchical supramolecular architectures are built from individual building blocks by a multi-level self-assembly process driven by noncovalent interactions.[5] However, in a crowded environment, like the inside of a cell, the effects that a hierarchical architecture experiences as a consequence of crowding, that is, the impact of depletion forces on the system, are easily overlooked.[6] In fact, the self-assembly process of biomolecules, such as nucleic acids and proteins, has been shown to be different under crowding conditions than in the dilute solutions usually used in sample preparation and analysis.[7] Intracellular macromolecules increase the effective concentration of protein monomers[8,9] and lower the critical concentration of the formation of cytoskeletal fibers.[10,11] Water-soluble non-adsorbing polymers are commonly used as crowding agents to induce depletion forces to mimic the crowding environment in vitro.[7] When placed in a crowding environment, biological filaments, such as the cytoskeleton, are inclined to align into highly ordered bundles and networks.[12,13] Even more, an active life-like hierarchical matter has been created upon the addition of molecular motors.[14,15]

In the field of synthetic molecules and materials, crowding effects have been explored to a much lesser extent,[7] even though the potential of depletion forces as a tool for constructing supramolecular materials has been demonstrated, for example, in the fields of lyotropic chromonic liquid crystals[16,17] and crystalline cellulose oligomer gels.[7,18] Intermolecular interactions may be affected by crowding conditions as demonstrated so far for a few peptide-based supramolecular assemblies[19–21] and diarylethene supramolecular fibers.[22] This handful of examples provides a tantalizing hint on what could be achieved by combining depletion interactions as an environmental control with precise molecular recognition. Utilizing strong specific interactions for stabilization of supramolecular assemblies aligned in a crowded environment has a potential to yield hierarchical organization across length scales beyond the control of molecular engineering.

F. Xiu, A. Knežević, J. Huskens, T. Kudernac
Molecular Nanofabrication Group
MESA+ Institute
University of Twente
PO Box 207, Enschede 7500 AE, The Netherlands
E-mail: t.kudernac@rug.nl
A. Knežević
Division of Organic Chemistry and Biochemistry
Ruđer Bošković Institute
Bijenička cesta 54, Zagreb 10000, Croatia
T. Kudernac
Faculty of Science and Engineering
Molecular Inorganic Chemistry
Stratingh Institute for Chemistry
Nijenborgh 4, Groningen 9747 AG, The Netherlands
The ORCID identification number(s) for the author(s) of this article can be found under https://doi.org/10.1002/smll.202207098.

DOI: 10.1002/smll.202207098

We demonstrate that exploiting the interplay between depletion forces and biomolecular recognition leads to the construction of stable microscopic and complex hierarchical architectures from molecular-sized building blocks. Depletion forces facilitate the bundling organization of artificial supramolecular polymers formed by the self-assembly process from small organic molecules. The crowding environment considerably influences the non-covalent interactions between supramolecular polymers, which is crucial for the formation of larger microscopic architectures. By employing strong cross-linking interactions between supramolecular polymers in a crowded environment in the form of multivalent biotin–streptavidin (SAv) conjugates as cross-linkers, robust microscopic structures are generated which are stable to resist dilution of crowded solutions.

2. Results and Discussion

2.1. Hierarchical Supramolecular Bundles Induced by Depletion Forces

Amphiphilic monomer **1**, bearing a V-shaped hydrophobic aromatic part and a hydrophilic branched oligo(ethylene glycol) unit (**Figure 1**), spontaneously assembles into stiff supramolecular tubes in water.[23] Here, poly(ethylene glycol) (PEG), a typical non-adsorbing, i.e., non-interacting, and very water-soluble polymer acting in water as coiled spheres, has been introduced into the solution of the supramolecular tubes to create a crowded environment. Isolated supramolecular tubes can be considered to be surrounded by an interspace inaccessible for the PEGs, called the "excluded volume."[24] By overlapping the polymer-inaccessible area of the tubes, the configurational entropy of the PEG crowding agent increases, and the total free energy of the whole system is decreased.[25–27] Thus, the assembled tubes experience a driving force making the tubes come closer to each other to minimize the excluded volume and permit the highest entropic freedom for the PEG (Figure 1, dashed line).[25] As a result, the supramolecular tubes form a hierarchical bundled architecture, leading to a much longer overlap length, stabilizing the whole self-assembled supramolecular system.

Microscopy provides evidence of crowding-induced fiber bundling. Individual supramolecular tubes of **1** assembled in an aqueous solution cannot be observed using optical microscopy due to the optical resolution limit (**Figure 2**A). Using electron microscopy tubular structures displaying random orientation can be observed (Figure 2B). Scanning electron microscopy (SEM) reveals tubes with a diameter of ≈10 nm, which is in agreement with earlier observations.[23] In contrast, distinct threadlike architectures with micron-sized diameter were observed by differential interference contrast (DIC) microscopy upon the addition of PEG (Figure 2C). This indicates that larger and thicker bundles composed of multiple, aligned tubes were formed in the solution. The morphology of the bundles was further confirmed by SEM (Figure 2D, Figure S1, Supporting Information). Both the DIC and SEM images indicate significant morphological and magnitude differences of architectures formed in water and in the PEG solution. The morphology of the network is visualized as a dense bundling structure when deposited on the substrate (Figure 2D). The difference in the prepared solutions is also evident to the naked eye. The mixed solution of **1** and PEG in water was turbid (Figure 2E, right), with subtle fibers visible in the sample, compared to the transparent solution of tubes in water with the same concentration of **1** (Figure 2E, left).

On the other hand, spectroscopic methods give an insight into what is happening within supramolecular tubes upon the

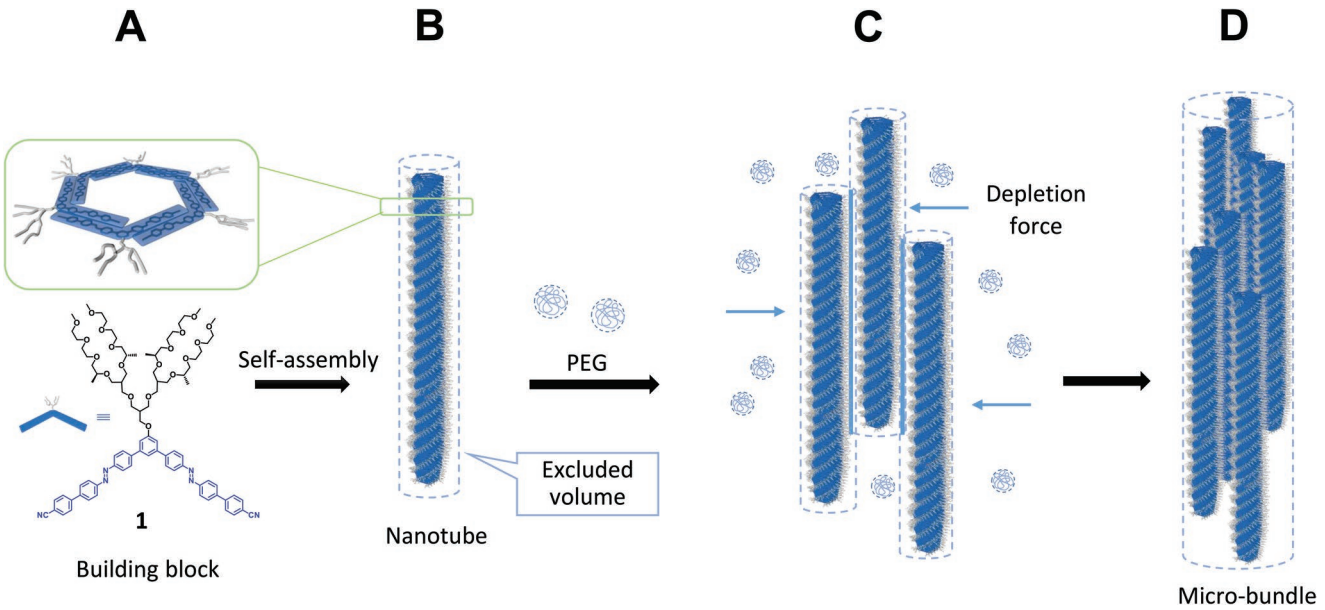

Figure 1. Schematic illustration of the depletion-induced hierarchical supramolecular bundling. A) Chemical structure of building block **1**. B) The self-assembly of the building blocks into supramolecular tubes. The excluded volume of the tube is illustrated with the dashed lines. C,D) Hierarchical supramolecular bundles induced by depletion forces in the PEG solution.

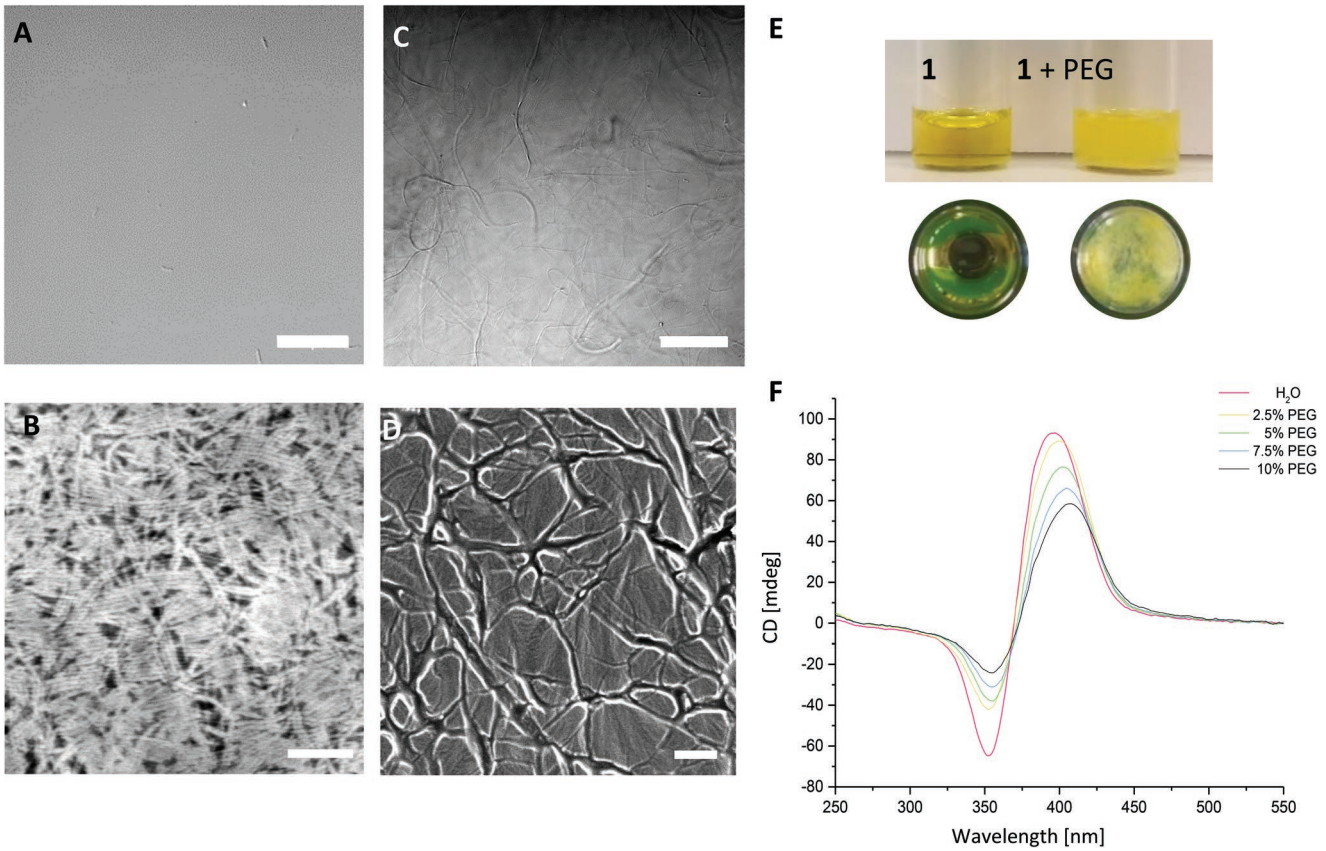

Figure 2. Comparing the morphology of tubes and micro-bundles formed by **1**. A) DIC image of tubes of **1** in the solution and B) SEM image of tubes of **1** (300 μm), C) DIC image of supramolecular bundles ([**1**] = 300 μm, 5% PEG) in the solution and D) SEM image of supramolecular bundles ([**1**] = 100 μM, 5% PEG). E) Comparison of tubes of **1** (300 μm) and upon addition of PEG (300 μm, 5% PEG). F) CD spectra of tubes of **1** (50 μm) in water and in PEG solutions at different PEG concentrations. Scale bars: (A), (C): 20 μm; (B): 100 nm, (D): 1 μm.

addition of PEG. The degree of the crowdedness of the system may affect the structure of the bundles as well as that of the assemblies within the bundles. Chiral tubes formed by **1** give a pronounced circular dichroism (CD) signal in water.[23] CD spectra of solutions of **1** (50 μm) differ in water and in the presence of PEG, and clearly depend on the concentration of PEG (Figure 2F). With the increase of the PEG concentration, with concomitantly increased crowding, the CD spectra showed a decreased intensity with steady UV spectra recorded simultaneously (Figure S2, Supporting Information). The UV absorbance slightly decreases only at higher PEG concentrations. Furthermore, at 50 μm of **1**, scarcely any microscopic-sized short bundles can be observed in DIC images regardless of the concentration of PEG (Figure S3, Supporting Information), resulting in clear solutions. The comparison of solutions at 2.5% and 5% PEG, where UV signal does not change while at the same time CD signal decreases significantly, indicates a decrease in helical chirality. This might be caused by the distortion of the tubes upon bundling. At the same time, the band shows a red-shift as the PEG concentration increases. This may be explained by a change of the π–π stacking interaction.[28,29] We speculate that the depletion forces and resulting bundling changes the local environment of the building blocks, allowing the overlapped π–π stacks to slip, which results in a red-shift of the absorption.[30]

On the structural level of the networks of bundles, a series of different concentrations of **1**-PEG solutions showed varying morphologies. It was found that the morphologies and dimensions of the observed bundles are related to the concentrations of both **1** and PEG (**Figure 3**A). Three types of structures were observed under the DIC microscope depending on the crowding degree—homogeneous solution (no distinct filaments seen under DIC which indicates the presence of only submicron tubes), micron-sized bundles (threadlike architectures with low contrast observed in DIC), and floccules (thicker fibers with higher contrast observed in DIC). At lower concentrations of **1**, a higher concentration of PEG is required to observe bundling, with no bundles found in the low PEG concentration region (Figure 3B). With the increase of the concentration of **1**, the minimum PEG content needed for detecting bundles became lower. At the same PEG concentration, thicker and larger-sized bundles were obtained by increasing the concentration of **1** (Figure 3C–F, Figure S4, Supporting Information). At 167 μm **1**, 3.3% PEG, fiber-like structures are faintly visible and thin. When the concentration of **1** was doubled (333 μm **1**, 3.3% PEG), distinct fiber-like bundles with larger sizes became visible. At even higher concentrations of PEG, thicker bundles appeared (Figure 3F). At high concentrations of both **1** and PEG, floating floccules were produced as a result of overcrowding. Under these conditions, bundles were pushed

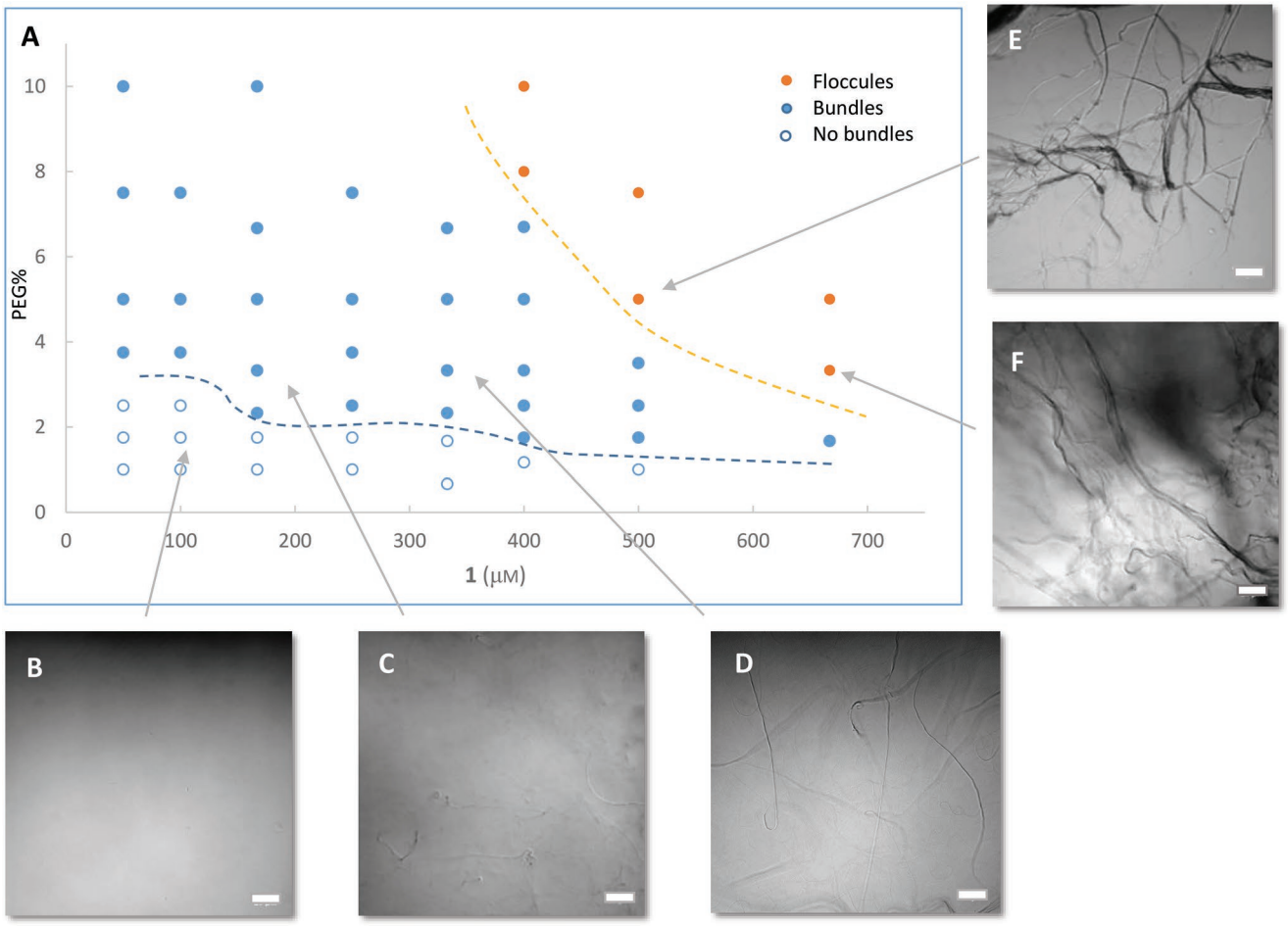

Figure 3. Phase diagram illustrating the effects of the concentrations of tubes and PEG on the assembled architectures. A) Phase diagram illustrating the effects of tubes and PEG concentration on assembled architecture. B–F) Each DIC image reveals a **1**-PEG mixture with various concentrations corresponding to an individual point in the diagram, showing its different features. Scale bar: 20 μm.

together to assemble into different networks or aggregates, thus providing clear trends as depicted in the constructed phase diagram (Figure 3A).

2.2. Engineering of Self-Assembled Architectures by the Interplay of Depletion Forces and Biomolecular Recognition

Given the bundle architecture can be controlled by crowding, we were interested to develop a strategy to lock and stabilize the microscopic bundled structures generated under the influence of depletion forces. Our idea was to utilize strong specific noncovalent interactions in combination with depletion forces. First, a small fraction (2%) of a biotinylated building block **2** was incorporated within the tubes of **1** (**Figure 4**). While the hydrophobic moiety of **2** is the same as in **1**, the hydrophilic section is altered into a single OEG chain with a terminal biotin group to allow strong interactions with tetravalent SAv protein. Building block **2** can co-assemble with **1** to generate supramolecular copolymer (**1–2**) tubes. The surfaces of these tubes are decorated with biotin. The final elongated tubes will have a certain number of binding sites along the tube, which can interact with SAv to form strong noncovalent crosslinked networks.[31] We expected that different assembled architectures could be formed by changing the order of non-covalent interactions implemented in the system, i.e., by changing the order of addition of the crowding agent and the SAv. Fluorescently labeled SAv was employed here to visualize its presence in the bundles and to indicate crosslinking using confocal laser scanning microscopy (CLSM) (Figure 4B,C). Tubes without biotinylated building block **2** do not form a supramolecular network upon the addition of SAv and homogenously distributed SAv is obtained (Figure S5, Supporting Information).

Equal volumes of 10% PEG solution and 2 μm SAv solution into the **1–2** supramolecular tubes solution (500 μm, **1**/**2** = 50) were mixed together. To understand the mutual influence of depletion forces and specific molecular interactions on the supramolecular architecture, we introduced the solutions in the above and in reverse order (Figure 4A). When PEG was added in the first step, long tight microscopic bundles were formed as previously described (Figure S6, Supporting Information). The morphology of these bundles did not change visibly upon the addition of SAv (Figure 4B). Fluorescent SAv became apparent in the fluorescence image and was concentrated along the backbone

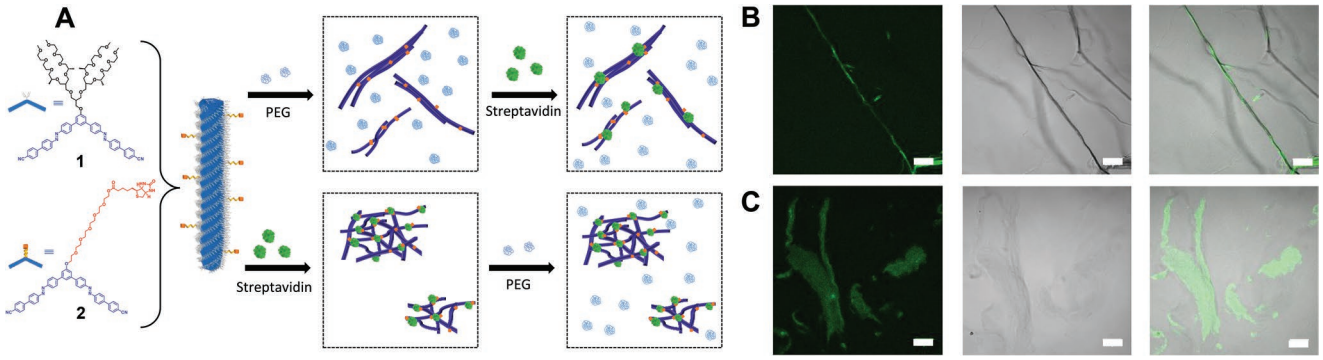

Figure 4. Microscopic architectures generated by the interplay of depletion forces and biomolecular recognition. A) Scheme demonstrating the assembly process induced by adding PEG and SAv in two different sequences. B) CLSM (left), DIC (middle), and merged images (right) of **1**–**2** (500 µm, **1**/**2** = 50) solution after addition of the same volumes of 10% PEG, followed by SAv-488 (2 µm) solution. C) **1**–**2** (500 µm, **1**/**2** = 50) solution after addition of the same volumes of SAv-488 (2 µm), followed by 10% PEG solution. Scale bars: 20 µm.

of the bundles as is evident from merged CLSM and DIC images. Apparently, the depletion-induced microscopic bundles formed by the addition of PEG were preserved when SAv was added. The SAv stained the bundles and interconnected them.

In contrast, porous crosslinked networks were produced by the addition of SAv to the solution of supramolecular tubes consisting of **1** and **2** (**1**/**2** = 50) (Figure 4C). These structures significantly differ in their morphology from the elongated bundles resulting from the addition of PEG. Once this crosslinking network was established by the strong biotin–SAv interactions, the morphology of the network remained intact after the addition of the PEG solution. This result indicates that once the crosslinked supramolecular network is formed, crowding effects have no further impact on the stable structure as a result of the specific and strong interactions. When depletion forces are employed in the first step, formed structures can be locked by implementing the strong interactions after the bundling, while if those interactions are present at the beginning, depletion forces have no further effect on the architecture. Thus, different and stable microscopic architectures can be created depending on the order of interactions implemented in the system.

2.3. Regulating Reversibility of Bundling by Biomolecular Interactions

To investigate the resistance of depletion-induced bundles and biotin–SAv-crosslinked bundles to dilution, these two types of bundles were diluted with water in the same dilution ratio to compare the resulting architectures. As discussed above, supramolecular tubes organize into micro-bundles induced by depletion forces, and the bundling architecture can be adjusted by varying the degree of crowding, i.e., by the PEG concentration. Microscale bundled architectures do not form in a dilute solution (Figure 3). This assembly of bundles is expected to be reversible between "crowded" and "diluted" (no PEG) solutions by modulating the PEG concentration. On the other hand, microscale bundles generated by depletion forces and further interconnected by strong specific (biotin–SAv) interactions, are expected to be more resistant under the same conditions.

In the absence of biotin–SAv crosslinks, the elongated bundles disappeared upon dilution as viewed under CLSM (**Figure 5**A). The **1**–**2** tubes dispersed from bundles into a diluted environment because the strength of the depletion forces was reduced due to the decrease of PEG concentration, thus removing the driving force for bundling. Subsequent addition of SAv resulted in the formation of complex network aggregates comprised of bundles and tubes (Figure S3, Supporting Information).

In contrast, persistent bundle structures were formed when biotin–SAv conjugates were used to stabilize depletion-induced bundles by adding SAv prior to dilution. These bundles remained intact in a solution that was diluted by a factor of three (Figure 5B). Clearly, the number of bundles decreased, but their form remained the same. The gray value profiles used for determining the diameter of bundles were measured before and after dilution for a set of bundles by CLSM (Figure 5C). The resulting bar graph showing the diameter distribution of the bundles (Figure 5D) reveals similar distributions before and after dilution, indicating that the dilution process has a limited effect on the diameter of bundles. This behavior suggests that biotin–SAv interactions produce persistent noncovalent crosslinking, which inhibits the bundles from reforming into scattered tubes upon dilution. On this basis, it is conceivable that bundle topologies created under certain crowding circumstances may be retained under more dilute settings when biotin-SAv is used for fixation.

3. Conclusion

As in biological systems, crowding effects play a significant role in the synthesis and characteristics of biomimetic supramolecular materials, whose use is expanding quickly. Thus, it is crucial to investigate the influence of a crowded environment on supramolecular assemblies. Here, we demonstrated that the morphology of hierarchical microscopic supramolecular structures generated in a solution is critically dependent on the degree of crowding governed by the PEG concentration. In addition, these tiny structures may be stabilized by the interplay of depletion forces and crosslinking through strong supramolecular interactions. In a solution of supramolecular polymers,

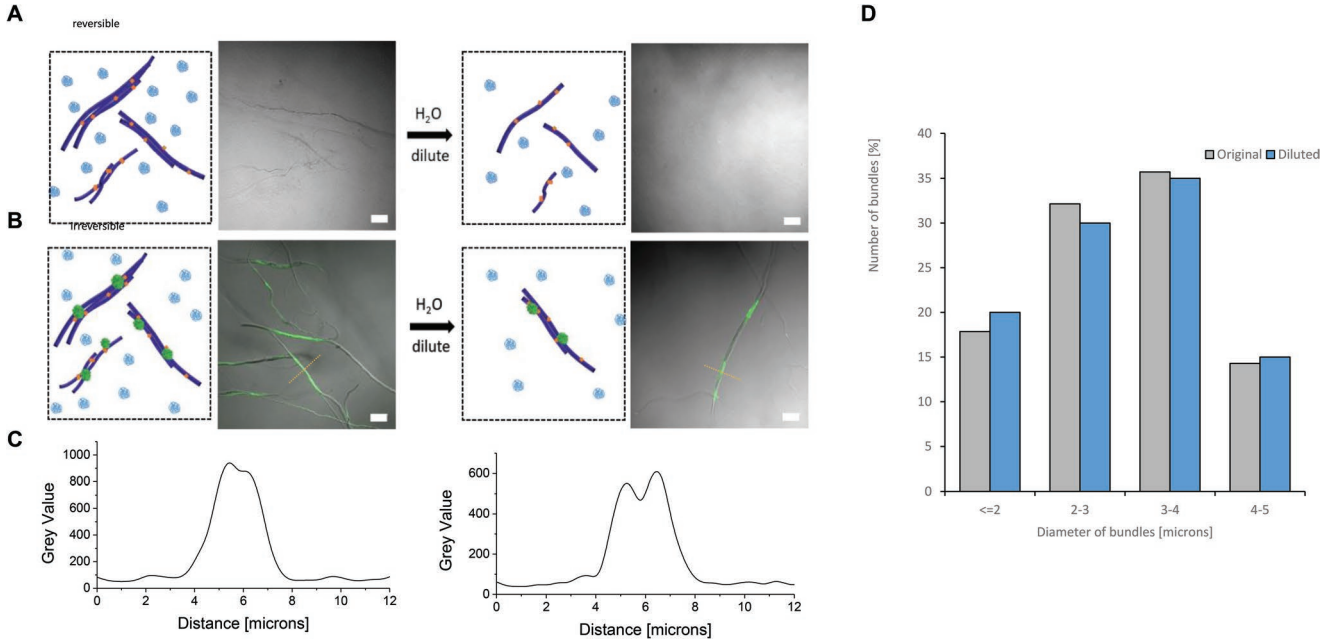

Figure 5. Dilution of microscopic bundles without and with stabilization with biotin-SAv. A) Left: bundles formed by mixing equal volume of 500 µm **1**–**2** (**1**/**2** = 50) tubes solution and 7.5% PEG solution. Right: After diluting with a factor 3. B) Left: bundles obtained as in (A) and fixed by adding fluorescent SAv-488 (2 µm) in the same volume as **1** and PEG solutions. Right: bundles after diluting with a factor 3. C) The gray value profile plot of the dashed lines of the fluorescent channel of the images of (B). D) Histogram of diameter distribution of bundles (process of (B), line profiles as in (C)) measured from CLSM.

depletion forces promote bundle formation, whereas strong non-covalent biotin–SAv interactions may be used to establish crosslinks between supramolecular polymers inside the bundle and "lock" the structure, making it stable against dilution. This strategy offers an approach for generating artificial cytoskeletal frameworks in a crowded aqueous environment.

4. Experimental Section

General: Poly(ethylene glycol) (PEG, M_w = 20 000) was purchased from Sigma-Aldrich and dissolved in MilliQ water to prepare PEG solutions. Alexa Fluor 488-labeled streptavidin (SAv) was purchased from Thermo Fisher Scientific Inc. SAv was dissolved in MilliQ water at a concentration of 1 mgmL^{-1}. Reagents and solvents were purchased from commercial sources and used without further purification. **1** and **2** were synthesized according to procedures reported previously.[23,31]

Preparation of the Samples: The solutions of **1** and multicomponent **1**–**2** samples were prepared from concentrated stock solutions of **1** (2 mM) and **2** (200 µm) in acetonitrile. Specific volumes of the concentrated stock solutions were mixed, and the solvent was evaporated in a nitrogen flow. The resulting residue was rehydrated in MilliQ water (200 µL) to reach the desired concentrations and left overnight before proceeding with experiments. The supramolecular bundles were prepared by mixing **1** and PEG solutions directly in a 1:1 volume ratio. The SAv was added after the bundle solution was premixed for 20 min.

Characterization: Scanning electron microscopy (SEM) samples were prepared by drop casting solutions without dilution on carbon grids (Formvar/carbon 200 mesh, copper). Prior to measurements, the samples were stained with 2% phosphotungstic acid for ≈30 s. The SEM images were then obtained with a Zeiss MERLIN HR-SEM. ImageJ software was used to analyze the SEM micrographs. The manual analysis led to the determination of the diameter of the tubes. Detailed information on determining the diameter of tubes using transmission electron microscopy, as well as the corroboration of results using the atomic force microscopy analysis, was previously reported.[23]

Circular dichroism (CD) spectrum measurements were carried out by using a Jasco J-1500 spectrometer, in the range of 300–600 nm, and at 20 °C in a nitrogen-filled chamber. The initial concentration of **1** solution was 100 µm. The samples were measured in 1 mm quartz cuvettes. The baseline spectra were measured in the same cuvettes filled with MilliQ water, and were subtracted from the sample spectra. The UV measurements were performed simultaneously using the same instrument.

Confocal laser scanning microscopy (CLSM, Nikon A1) and differential interference contrast (DIC) microscopy (Nikon A1) were used to observe the **1** and **1**–**2** bundles freely floating in solutions, without immobilization. The Alexa Fluor 488-labeled SAv was examined by CLSM with an excitation wavelength of 488 nm. ImageJ software was used to analyze the CLSM micrographs to determine the diameter of the bundles.

Supporting Information

Supporting Information is available from the Wiley Online Library or from the author.

Acknowledgements

F.X. and A.K. contributed equally to this work. This project was received funding from the European Union's Horizon 2020 research and innovation programme under the Marie Skłodowska-Curie grant agreement No. 841150, SHINEShift granted to A.K.. T.K. thanks the European Research Council (ERC Consolidator Grant, MechanoTubes, 819075) for funding. F.X. acknowledges China Scholarship Council (CSC) for the financial support. The authors thank Enrico G. Keim for TEM measurements and Mark A. Smithers for SEM measurements.

Conflict of Interest

The authors declare no conflict of interest.

Data Availability Statement

The data that support the findings of this study are available from the corresponding author upon reasonable request.

Keywords

depletion forces, helical structures, hierarchical architectures, noncovalent interactions, self-assembly

Received: November 22, 2022
Revised: January 27, 2023
Published online: February 25, 2023

[1] C. Yuan, W. Ji, R. Xing, J. Li, E. Gazit, X. Yan, *Nat. Rev. Chem.* **2019**, *3*, 567.
[2] P. J. Horn, C. L. Peterson, *Science* **2002**, *297*, 1824.
[3] A. Gautieri, S. Vesentini, A. Redaelli, M. J. Buehler, *Nano Lett.* **2011**, *11*, 757.
[4] M. J. Buehler, *Proc. Natl. Acad. Sci. U. S. A.* **2006**, *103*, 12285.
[5] G. M. Whitesides, B. Grzybowski, *Science* **2002**, *295*, 2418.
[6] D. Marenduzzo, K. Finan, P. R. Cook, *J. Cell Biol.* **2006**, *175*, 681.
[7] Y. Hata, T. Sawada, T. Serizawa, *J. Mater. Chem. B* **2018**, *6*, 6344.
[8] D. Popp, R. C. Robinson, *Cytoskeleton* **2012**, *69*, 71.
[9] A. P. Minton, *J. Biol. Chem.* **2001**, *276*, 10577.
[10] A. P. Minton, *Curr. Opin. Struct. Biol.* **2000**, *10*, 34.
[11] T. L. Madden, J. Herzfeld, *Biophys. J.* **1993**, *65*, 1147.
[12] R. Tharmann, M. M. A. E. Claessens, A. R. Bausch, *Biophys. J.* **2006**, *90*, 2622.
[13] K. Okeyoshi, R. Kawamura, R. Yoshida, Y. Osada, *Sci. Rep.* **2015**, *5*, 9581.
[14] T. Sanchez, D. Welch, D. Nicastro, Z. Dogic, *Science* **2011**, *333*, 456.
[15] T. Sanchez, D. T. N. Chen, S. J. DeCamp, M. Heymann, Z. Dogic, *Nature* **2012**, *491*, 431.
[16] L. Tortora, H.-S. Park, S.-W. Kang, V. Savaryn, S.-H. Hong, K. Kaznatcheev, D. Finotello, S. Sprunt, S. Kumar, O. D. Lavrentovich, *Soft Matter* **2010**, *6*, 4157.
[17] H.-S. Park, S.-W. Kang, L. Tortora, S. Kumar, O. D. Lavrentovich, *Langmuir* **2011**, *27*, 4164.
[18] Y. Hata, T. Kojima, T. Koizumi, H. Okura, T. Sakai, T. Sawada, T. Serizawa, *ACS Macro Lett.* **2017**, *6*, 165.
[19] A. Restuccia, D. T. Seroski, K. L. Kelley, C. S. O'Bryan, J. J. Kurian, K. R. Knox, S. A. Farhadi, T. E. Angelini, G. A. Hudalla, *Commun. Chem.* **2019**, *2*, 53.
[20] M.d. M. Hassan, A. D. Martin, P. Thordarson, *J. Mater. Chem. B* **2015**, *3*, 9269.
[21] N. Javid, S. Roy, M. Zelzer, Z. Yang, J. Sefcik, R. V. Ulijn, *Biomacromolecules* **2013**, *14*, 4368.
[22] A. Sakaguchi, K. Higashiguchi, K. Matsuda, *Chem. Commun.* **2018**, *54*, 4298.
[23] J. W. Fredy, A. Méndez-Ardoy, S. Kwangmettatam, D. Bochicchio, B. Matt, M. C. A. Stuart, J. Huskens, N. Katsonis, G. M. Pavan, T. Kudernac, *Proc. Natl. Acad. Sci. U. S. A.* **2017**, *114*, 11850.
[24] M. Braun, Z. Lansky, F. Hilitski, Z. Dogic, S. Diez, *BioEssays* **2016**, *38*, 474.
[25] J. Schnauß, T. Händler, J. Käs, *Polymers* **2016**, *8*, 274.
[26] M. Hosek, J. X. Tang, *Phys. Rev. E* **2004**, *69*, 051907.
[27] S. Asakura, F. Oosawa, *J. Chem. Phys.* **1954**, *22*, 1255.
[28] X. Cao, L. Meng, Z. Li, Y. Mao, H. Lan, L. Chen, Y. Fan, T. Yi, *Langmuir* **2014**, *30*, 11753.
[29] W.-J. Wang, L. Hao, C.-Y. Chen, Q.-M. Qiu, K. Wang, J.-B. Song, H. Li, *RSC Adv.* **2017**, *7*, 20488.
[30] Z. Huang, S.-K. Kang, M. Banno, T. Yamaguchi, D. Lee, C. Seok, E. Yashima, M. Lee, *Science* **2012**, *337*, 1521.
[31] F. Xiu, A. Knežević, S. Kwangmettatam, D. Di Iorio, J. Huskens, T. Kudernac, *Adv. Mater.* **2022**, *34*, 2105926.